

## RESEARCH LETTER

10.1029/2018GL077946

### Key Points:

- Warming and inhibition of salinization of the sea surface are controlled by cyanobacterial surface blooms
- In the absence of surface blooms, skin layer is generally cooler and saltier
- A new phenomenon of “apparent” freshening of the sea surface is described, which has been assumed to occur only by precipitation

### Supporting Information:

- Supporting Information S1

### Correspondence to:

O. Wurl,  
oliver.wurl@uni-oldenburg.de

### Citation:

Wurl, O., Bird, K., Cunliffe, M., Landing, W. M., Miller, U., Mustaffa, N. I. H., et al. (2018). Warming and inhibition of salinization at the ocean's surface by cyanobacteria. *Geophysical Research Letters*, 45, 4230–4237. <https://doi.org/10.1029/2018GL077946>

Received 27 NOV 2017

Accepted 26 APR 2018







Accepted article online 2 MAY 2018

Published online 12 MAY 2018

©2018. The Authors.

This is an open access article under the terms of the Creative Commons Attribution-NonCommercial-NoDerivs License, which permits use and distribution in any medium, provided the original work is properly cited, the use is non-commercial and no modifications or adaptations are made.

## Warming and Inhibition of Salinization at the Ocean's Surface by Cyanobacteria

O. Wurl<sup>1</sup> , K. Bird<sup>2</sup> , M. Cunliffe<sup>2,3</sup>, W. M. Landing<sup>4</sup> , U. Miller<sup>5</sup>, N. I. H. Mustaffa<sup>1</sup> , M. Ribas-Ribas<sup>1</sup> , C. Witte<sup>5</sup> , and C. J. Zappa<sup>5</sup> 

<sup>1</sup>Institute for Chemistry and Biology of the Marine Environment, Carl von Ossietzky University Oldenburg, Wilhelmshaven, Germany, <sup>2</sup>Marine Biological Association of the United Kingdom, Plymouth, UK, <sup>3</sup>Marine Biology and Ecology Research Centre, School of Biological and Marine Sciences, Plymouth University, Drake Circus, Plymouth, UK, <sup>4</sup>Department of Earth, Ocean, and Atmospheric Science, Florida State University, Tallahassee, FL, USA, <sup>5</sup>Lamont-Doherty Earth Observatory, Columbia University, Palisades, NY, USA

**Abstract** This paper describes high-resolution in situ observations of temperature and, for the first time, of salinity in the uppermost skin layer of the ocean, including the influence of large surface blooms of cyanobacteria on those skin properties. In the presence of the blooms, large anomalies of skin temperature and salinity of 0.95°C and −0.49 practical salinity unit were found, but a substantially cooler (−0.22°C) and saltier skin layer (0.19 practical salinity unit) was found in the absence of surface blooms. The results suggest that biologically controlled warming and inhibition of salinization of the ocean's surface occur. Less saline skin layers form during precipitation, but our observations also show that surface blooms of *Trichodesmium* sp. inhibit evaporation decreasing the salinity at the ocean's surface. This study has important implications in the assessment of precipitation over the ocean using remotely sensed salinity, but also for a better understanding of heat exchange and the hydrologic cycle on a regional scale.

**Plain Language Summary** We provide high-resolution in situ observations of large cyanobacterial blooms floating in a biofilm-like microlayer on the ocean's surface. Our observations show biologically controlled warming and freshening of the surface by the surface blooms that are essential in understanding global heat exchange and the hydrologic cycle. Our study describes a new phenomenon to force “apparent” freshening of the sea surface—in the literature assumed to occur only by precipitation. It further challenges the development of algorithms and validation of remotely sensed temperature and salinity from space. Our finding of active microbial communities in the sea surface microlayer highlights the sea surface as another environment for extreme habitats and microbial adaptation. Our discovery of their influence on satellite observations of sea surface temperature and salinity is fundamental for future research in remote sensing, marine microbiology, air-sea interaction, and climate regulation.

## 1. Introduction

Satellite observations of climate variables in the ocean are crucial to understand the magnitude of the global water cycle, ocean circulation, primary productivity, and climate change (Martin, 2014). Cyanobacteria are photosynthetic microorganisms that can significantly increase in abundance (bloom) at the ocean's surface and become visible from space (Capone et al., 1997), and also change the physical features of the sea surface (Frka et al., 2012). Floating cyanobacteria colonies are embedded in a gelatinous matrix sharing properties with biofilms, and subsequently form visibly smooth patches, also known as slicks, caused by capillary wave damping (Wurl et al., 2016). Cyanobacteria slicks exhibit significant effects on the sea surface temperature (SST) and heat exchange between the ocean and atmosphere (Kahru et al., 1993).

The effects of slicks on SST include different emissivity of slicks and nonslick surfaces based on investigations of artificial oil films (Zhou et al., 2017), decrease of evaporation rates (La Mer & Healy, 1965), and additional layer thickness due to reduced turbulence in the absence of capillary waves (Saunders, 1967). An increase of SST by 1.5°C has been observed in the presence of large cyanobacterial surface blooms in the Baltic Sea (Kahru et al., 1993) due to enhanced solar absorption by cyanobacteria. The prediction of SST in the presence of slicks, however, remains uncertain as slicks not induced by cyanobacteria have a cooling signature compared to the SST of ambient water surfaces (Marmorino & Smith, 2006). Such knowledge is essential for the evaluation of satellite observations because of the frequent appearance (Romano, 1996) and large size

(up to 1,300 km<sup>2</sup>) of slicks (Capone et al., 1998; Kahru et al., 1993). Slicks induced by the large filamentous cyanobacterium *Trichodesmium* sp. have been reported during calm sea states in tropical regions (Capone et al., 1998; Sieburth & Conover, 1965; Wurl et al., 2011). So far, no observations have been published for the magnitude and direction of associated salinity anomalies. Salinity of the skin layer is forced by evaporation and precipitation (Soloviev & Lukas, 2006), and model approaches have shown salinity anomalies of 0.15 to 0.25 practical salinity unit (PSU; Song et al., 2015; Yu, 2010; Zhang & Zhang, 2012).

Here we show, using high-resolution in situ measurements, that slicks formed by cyanobacteria both warm the upper <1 mm of the ocean's surface compared to the near-surface mixed layer and inhibit salinization of the ocean's surface. Considering that the ocean absorbs 90% of the "anthropogenic" heat trapped by greenhouse gases (Levitus et al., 2012), these observations of biologically controlled warming and inhibition of salinization of the surface are essential in understanding heat exchange, the development of algorithms to reliably interpret SST and sea surface salinity (SSS) from satellites, and ultimately in the prediction of regional warming.

## 2. Methods

Observations were made in the Indo-West Pacific during cruise FK161010 (11 October to 10 November 2016; R/V Falkor). Similar to earlier observations from the Sargasso Sea (Sieburth & Conover, 1965), we observed patchy and banded slicks of cyanobacterial surface blooms (Figure S1) in the Joseph Bonaparte Gulf (Timor Sea; centered at 12.45°S, 126.62°E) over several hours on the 14 and 15 October 2016 (UTC).

The thermal boundary layer has been reported to vary between 500 and 1,000  $\mu\text{m}$  in thickness (Donlon et al., 2002). The thickness of the salinity boundary layer is 200  $\mu\text{m}$  thick due to different diffusivity scaling relationships (Katsaros, 1980). SST, SSS (derived from conductivity), and fluorescent dissolved organic matter (FDOM) were measured in a layer of  $\sim 80$   $\mu\text{m}$  thickness with a rotating glass disk sampler mounted on the remote-controlled catamaran Sea Surface Scanner (S<sup>3</sup>; Ribas-Ribas et al., 2017). The 80- $\mu\text{m}$  layer adheres to the disks through surface tension, is removed from the ascending side of the disk assembly by wipers, and pumped through onboard sensors. We estimate a time delay of approximately 7 s for water adhering to the disks to enter the pump tubing, protected from direct exposure of solar radiation, considering the following: (i) rotational speed of the disks of approximately 8 s per rotation, (ii) the fact that the disks are immersed to a depth equivalent to about one third of their diameter ( $8 \text{ s} * 0.66 = 5.3 \text{ s}$ ), and (iii) run-off time from the wipers of 2 s resulting in the time delay of 7 s. The disks are shaded by a low-transmitting dark-colored shield, and their positions between the hulls minimize the warming of the disks and adhering water as well evaporative cooling. In addition, continuous immersion prevents warming of the disks.

Simultaneously, temperature, salinity, and FDOM were measured at 1 m depth, from which  $\Delta S = S_{S3} - S_{1m}$  and  $\Delta T = T_{S3} - T_{1m}$  were determined.  $S_{S3}$  and  $T_{S3}$  are the average salinity and temperature measured in the top 80  $\mu\text{m}$  of the sea surface skin layer, respectively. The accuracy of the temperature and conductivity sensors was  $\pm 0.1^\circ\text{C}$  and  $\pm 0.2\%$ , respectively (Ribas-Ribas et al., 2017). The enrichment factor (EF) of FDOM was calculated as the ratio between the concentrations in the skin to that of the corresponding water sample from 1 m depth. Data were logged with a frequency of 0.1 Hz, and averaged over each minute of operation. The meteorological and radiation sensors, including wind speed, air temperature, and humidity, were mounted on the catamaran mast at a height of 3 m above the sea surface.

The temperature difference across the skin layer,  $\Delta T_{\text{skin}}$ , is the skin SST minus the subskin SST (Jessup et al., 2009). The skin SST is defined as the radiometric temperature measured across a very small depth of approximately 20  $\mu\text{m}$ . The subskin SST represents the temperature at the base of the thermal skin layer. Skin SST was determined by an infrared (IR) camera installed on the upper deck of the research vessel Falkor along with downward and upward looking IR radiometers. The Stirling-cycle cooled IR camera imagery measured thermal radiation from 7.7 to 9.3  $\mu\text{m}$  emitted by the ocean surface (and reflected by the sky), and brightness temperature was obtained with a resolution of  $0.02^\circ\text{C}$  (noise-equivalent temperature difference). Calibration with a blackbody was better than  $\pm 0.05^\circ\text{C}$  (Zappa et al., 2012). Brightness temperature was measured by IR imagery at a sampling rate of 100 Hz in 20-min bursts and was measured by IR radiometry at a sampling rate of 1 Hz continuously. The radiometer is calibrated with the same blackbody to  $\pm 0.1^\circ\text{C}$ . Both the IR camera and radiometer were corrected for sky reflection (Donlon et al., 2014; Katsaros, 1980) by an upward

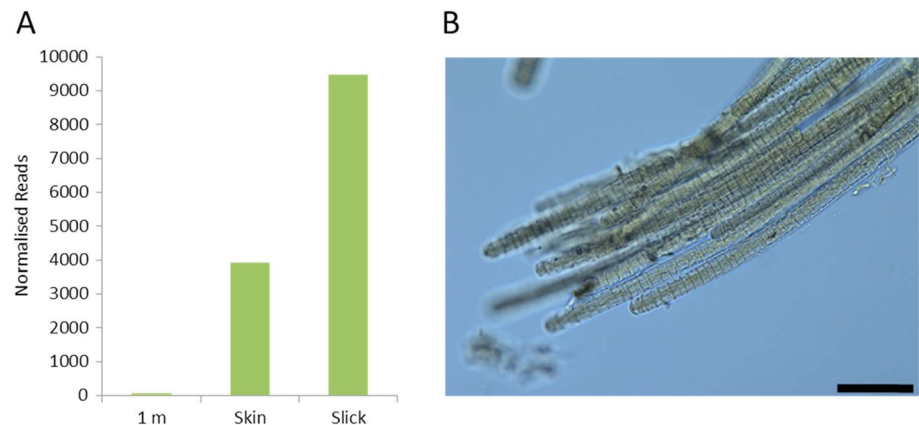


**Figure 1.** (a) *Trichodesmium* sp. abundance as the number of normalized bacterial 16S rRNA genes (Normalized Reads) in manual samples taken at 04:15 UTC (15 October 2016) from 1 m below the surface, the surface skin, and surface slick. Note that the skin sample was collected between the surrounding banded slicks and cannot be considered as a “clean” skin layer. (b) Micrograph of sampled colonies of *Trichodesmium* sp. Scale bar represents 50 μm.

looking radiometer to estimate the skin SST using known emissivity values for the ocean surface (Downing and Williams, 1975). The difference between the skin and subskin SST,  $\Delta T_{\text{skin}}$ , was calculated directly using the distribution of temperature measured by the IR imager (Jessup et al., 2009), under the assumption that turbulent renewal of the skin layer leads to sampling a range of skin and subskin thermal values. This technique precludes the need for knowledge of the sky reflection. Polarimetric imaging (Zappa et al., 2008; Zappa et al., 2012) from the upper deck of the *R/V Falkor* provided a visible reference of the ocean surface.

In summary, temperature and salinity in the upper 80 μm were measured from the catamaran  $S^3$  ( $T_{S3}$  and  $S_{S3}$ , respectively), and temperature and salinity anomalies calculated from the reference bulk temperature and salinity at 1 m depth, i.e.,  $\Delta T = T_{S3} - T_{1m}$  and  $\Delta S = S_{S3} - S_{1m}$ , respectively. Temperature in the upper 20 μm was measured by an IR camera (skin SST), and its anomaly across the thermal skin layer (approximately the upper 1000 μm) refers to  $\Delta T_{\text{skin}}$ .

*Trichodesmium* sp. abundance was determined by bacterial 16S rRNA gene high-throughput sequencing. In brief, 0.5 L seawater was sampled from the skin layer using a glass plate (Harvey & Burzell, 1972) and from 1 m below the surface. Samples were filtered onto 0.2 μm membrane filters and stored in RNeasy Lysis Buffer (Qiagen, UK) at  $-80^{\circ}\text{C}$ . DNA was later extracted using a commercially available DNeasy kit (Qiagen, UK). 16S rRNA gene library preparation and sequencing were performed at the Integrated Microbiome Resource at the Centre for Comparative Genomics and Evolutionary Bioinformatics, Dalhousie University (Comeau et al., 2017). Sequences were analyzed in QIIME as previously described (Taylor et al., 2014). Slicks were dominated by a single operational taxonomic unit (OTU3), which was identified as *Trichodesmium* sp. using the National Center for Biotechnology Information BLAST database.

The statistical analysis was performed with GraphPad PRISM version 5.0. Correlation tests were based on Spearman's correlation coefficient and 95% confidence intervals (CIs). All other values were reported as average  $\pm$  standard deviation based on repeated measurements.

### 3. Results and Discussion

We identified the cyanobacterium *Trichodesmium* sp. in extremely high abundance in skin samples from slick areas compared to nonslick and underlying water samples (Figure 1).

The EF of FDOM is used as proxy for the presence of slicks (Frew et al., 2004), and Figure 2 shows that slicks appeared after 01:16 UTC (local time is nine and a half hours ahead).

Positive  $\Delta T$  (i.e., warmer sea surface) and negative  $\Delta S$  (i.e., fresher sea surface) were coincident with slicks (Figure 2). This measured positive  $\Delta T$  is due to the presence of the surface slick. To demonstrate the role of

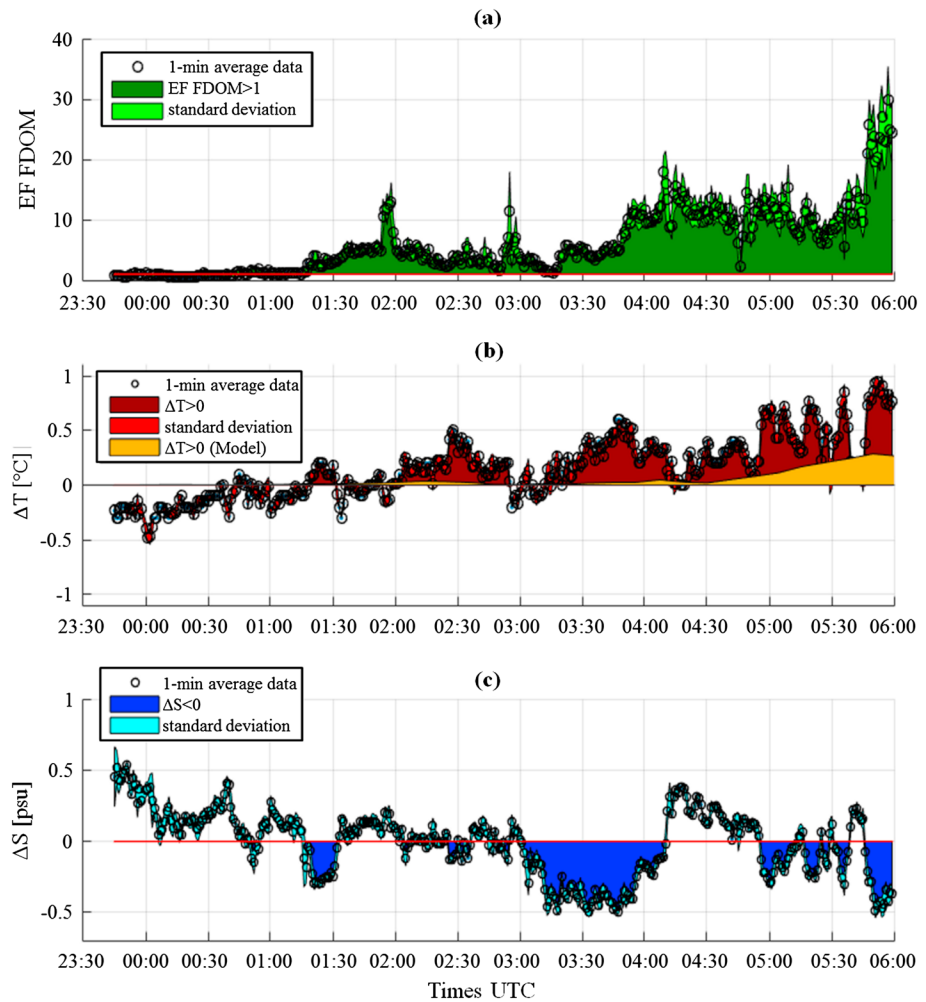


**Figure 2.** Time series from 23:45 UTC (14 October 2016) to 05:59 UTC (15 October 2016). (a) Enrichment factor (EF) of fluorescent dissolved organic matter (FDOM; the dark green areas indicate the presence of slicks), (b) temperature anomaly ( $\Delta T$ ; the dark red areas indicate the in situ warm surface layer; the orange areas indicate the model surface layer warming according to Price et al., 1986, and noted as Price Weller Pinkel [PWP] for short throughout), and (c) salinity anomaly ( $\Delta S$ ; the dark blue areas indicate the fresher surface layer). Standard deviations are from 1-min averaged data, and the averaged data are represented by black circles.

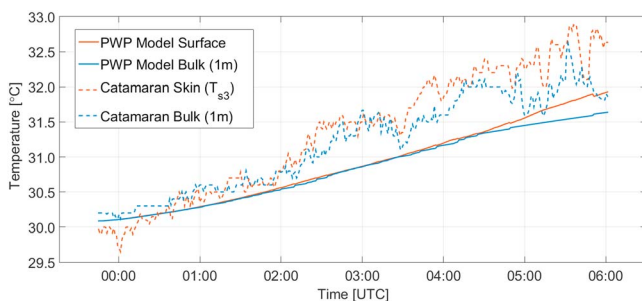


**Figure 3.** Time series of the in situ temperature measurements from the catamaran (skin  $T_{s3}$  and 1 m bulk) and the PWP modeled temperatures (surface and 1 m).

the slick, we ran a one-dimensional diurnal mixed-layer model (Price et al., 1986; Price Weller Pinkel model or in short PWP) that accounts for solar absorption without the impact of surface slicks. In contrast to the observations (Figure 2b), only modest warming occurred in the model, and this was delayed relative to the observations by more than 2 hr. The largest anomalies of  $\Delta T$  (in situ: 0.95°C at 05:52 UTC; model: 0.30°C at 05:50 UTC; Figure 2b) and  $\Delta S$  (−0.50 PSU at 03:47 UTC, and −0.49 PSU at 05:51 UTC; Figure 2c) occurred with the largest FDOM enrichments at the surface (EF = 4.90 at 03:47 UTC and EF = 20.44 at 05:52 UTC; Figure 2a). Furthermore, Figure 3 demonstrates that while both the in situ temperatures ( $T_{s3}$  and 1 m bulk) and the modeled temperatures (surface and 1 m) both increase, the in situ temperatures in the upper 80- $\mu$ m layer ( $T_{s3}$ ) and 1 m bulk water warm more quickly.

While FDOM enrichment in slicks collected by  $S^3$  generally yielded a less saline skin layer, high FDOM enrichments between 04:00 UTC



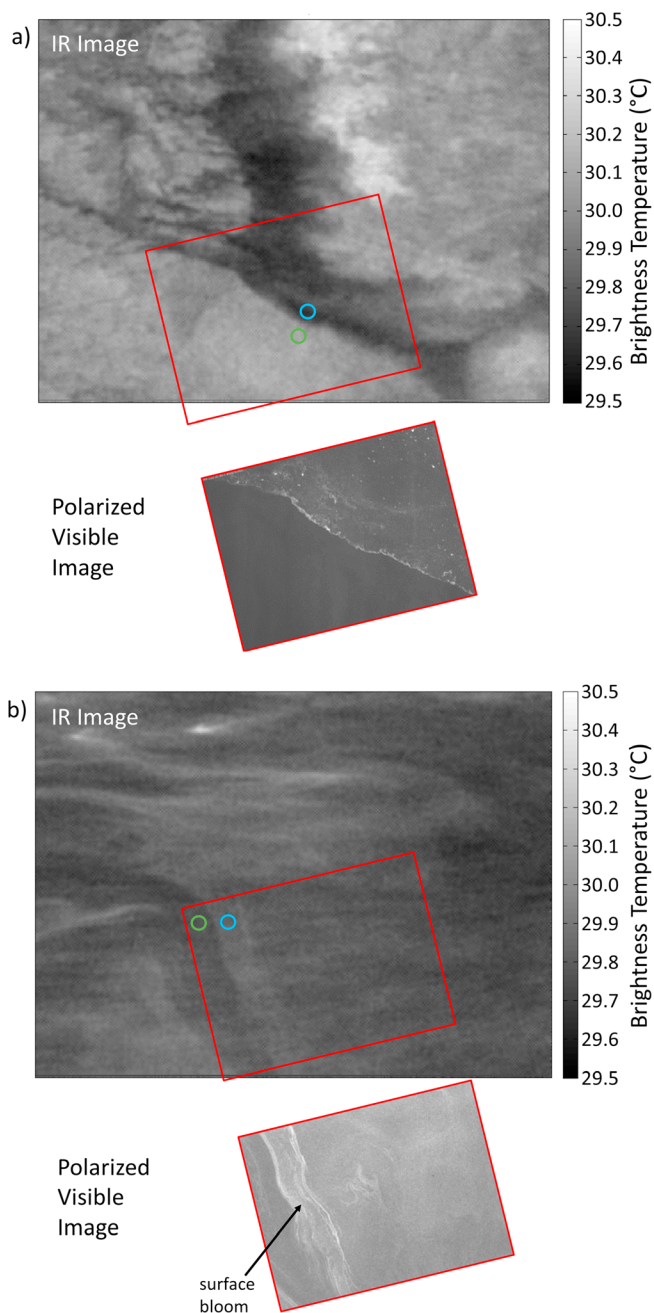


**Figure 4.** Infrared images ( $3.50 \text{ m} \times 2.75 \text{ m}$ ) showing sea surface brightness temperature with bright areas warmer and dark areas cooler, and polarized visible images ( $1.0 \text{ m} \times 0.8 \text{ m}$ ). (a) Slick without cyanobacterial bloom showing cooler skin layer, for example, negative in situ  $\Delta T$  from  $5^{\circ}\text{C}$  (02:56 UTC, 15 October 2016; see Figure 2). For the noncyanobacterial slick, the brightness temperature in the slick is  $29.68^{\circ}\text{C} \pm 0.02^{\circ}\text{C}$  (blue circle) and outside is  $30.10^{\circ}\text{C} \pm 0.02^{\circ}\text{C}$  (green circle). (b) Slicks associated with cyanobacterial blooms show a warmer skin layer, for example, positive in situ  $\Delta T$  (02:24 UTC, 15 October 2016). For the cyanobacteria slick, the brightness temperature in the slick is  $29.84^{\circ}\text{C} \pm 0.02^{\circ}\text{C}$  (blue circle) and outside is  $29.77^{\circ}\text{C} \pm 0.02^{\circ}\text{C}$  (green circle).

and 04:30 UTC corresponded to a more saline skin layer. Other processes such as dynamic evaporation and associated cooling, thinning of the skin layer by wind-driven dispersion, and photo degradation of FDOM in the skin layer are likely to have contributed to this observation. Both the skin temperature and, to a lesser extent, the subsurface temperature increased and led to the positive  $\Delta T$  (Figure 3), which deviated less from the FDOM trend than  $\Delta S$ . Our observation on the greatest degree of warming of the sea surface by  $0.95^{\circ}\text{C}$  is consistent with observations by satellite-based radiometers of regions ( $>1,000 \text{ km}^2$ ) warmer by  $1.5^{\circ}\text{C}$ , supposedly caused by cyanobacterial surface blooms and supported by opportunistic ship measurements (Kahru et al., 1993). Without the presence of slicks, we observed a cooler surface (averaged  $-0.22 \pm 0.09^{\circ}\text{C}$ ; Figure 2b) consistent with numerous reports on the “cool skin layer” (Soloviev & Lukas, 2006).

Interestingly, natural slicks that are not associated with cyanobacterial blooms often have a cooler skin, typically  $0.1$  to  $0.4^{\circ}\text{C}$  compared to ambient nonslick surfaces as observed using aircraft-based IR radiometers (Marmorino & Smith, 2006). Laboratory measurements have shown cool skin layers for varying surfactants, depending on their ability to modulate evaporation, lower surface tension, or change viscosity and therefore alter convective mixing with underlying bulk water (Jarvis, 1962). The IR and polarimetric imagery shows cooling of the skin layer in the presence of slicks without cyanobacteria (Figure 4a). The measurements of skin SST by both IR radiometry and IR imagery is compared in Figure 5 with the in situ skin layer temperature from the catamaran. The two distributions of skin SST are comparable, but the in situ skin layer temperature shows a tendency to warmer temperatures. The skin SST is measured in the top  $20 \mu\text{m}$  of the surface in contrast to the in situ skin layer temperature that is measured in the top  $80 \mu\text{m}$ . Furthermore, our measurements from nonslick areas demonstrate the skin SST to be always lower than the subskin SST (see Figure 2b; 23:45 UTC to 01:15 UTC). The cooling effect is in line with the increased thickness of the thermal conduction layer induced by the wave-damping phenomena reducing near-surface turbulence (McLeish & Putland, 1975). In contrast, slicks may also inhibit evaporation due to a close packed monomolecular film (La Mer & Healy, 1965) and/or, a gel-like matrix (Wurl et al., 2016), which could also include monomolecular surface films. The inhibition of evaporation reduces the heat loss from the sea surface and therefore partly offsets the cooling effect. The combination of multiple effects of slicks on evaporation and near-surface turbulence, for example, thickening thermal boundary layer, existence of closely packed monolayers, and type of surfactants, is a poorly understood process. However, due to the existence of cool slicks of noncyanobacterial origin (Marmorino & Smith, 2006), inhibition of evaporation will only influence the cool skin effect.

For the IR imagery in Figure 4 of the noncyanobacterial slick, the brightness temperature signature of a cooler slick is comparable with previous observations of cooler surface slicks. For the slicks associated with cyanobacterial blooms, the observations of warming are real

rather than apparent since any changes in emissivity should have minimal impact, or cooling effect, on the brightness temperature. Hühnerfuss et al. (1986) state that monomolecular surface films do not change the emissivity of the sea surface significantly in contrast to crude-oil films (Grossman et al., 1969; Jarvis &

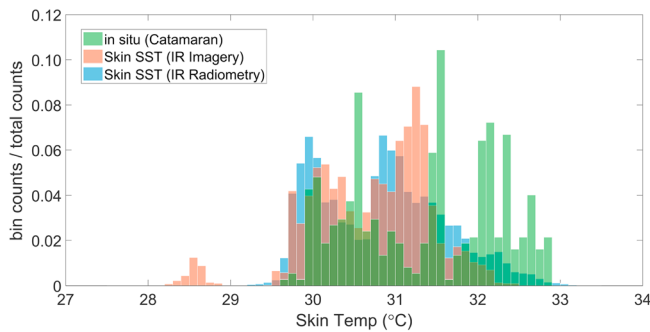


**Figure 5.** Distribution of skin SST (upper 20  $\mu\text{m}$ ) by both IR radiometry and IR imagery in comparison with the in situ 80- $\mu\text{m}$ -layer temperature  $T_{S3}$  from the catamaran  $S^3$ .

Kagarise, 1962). We conclude that the observed warming is directly linked to the cyanobacterial-dominated slicks as shown by the IR and polarimetric imagery (Figure 4b).

Mycosporine-like amino acids are common cyanobacteria pigments (Sinha et al., 1998) that are present in higher concentrations at the ocean's surface (Tilstone et al., 2010), and are known to dissipate 97% of the adsorbed energy to the surroundings as heat (Conde et al., 2004). Cyanobacteria are also known to excrete the extracellular pigments Scytonemin and Gloeocapsin (Sinha et al., 1998) into the ambient gel-matrix. Our slick samples showed more pronounced rose coloration (Figure S2), which indicates synthesis and excretion of the pigment Gloeocapsin (Sinha et al., 1998) by the slick communities. High solar radiation causes strong stratification and traps cyanobacteria close to the surface by losing their buoyancy regulation, a phenomenon called inverted sedimentation (Kahru et al., 1994). As a positive feedback loop, warming of the microlayer is intensified by the synthesis and excretion of pigments on the ocean's surface resulting from the massive surface accumulation of cyanobacteria (Kahru et al., 1994).

Previous studies have assumed that freshening of the ocean's surface occurs only by precipitation (Soloviev & Lukas, 2006); however, we report that slicks also inhibit salinization and produce an apparent freshening. As mentioned above, closely packed monomolecular films retard evaporation from water surfaces, and more disorganized films with complex mixtures of substances retain the capability to reduce evaporation rates (La Mer & Healy, 1965) causing a fresh salinity anomaly ( $\Delta S < 0$ ). We obtained a significant and strong correlation between  $\Delta T$  and EF FDOM ( $r = 0.708$ , 95% CI [0.663, 0.748],  $n = 374$ ), but EF FDOM correlated only weakly with  $\Delta S$  ( $r = -0.270$ , 95% CI [-0.347, -0.189],  $n = 374$ ; Figure S3). Considering only data in the presence of cyanobacterial slicks, the correlation even weakened in both cases for  $\Delta T$  ( $r = 0.420$ , 95% CI [0.336, 0.498],  $n = 284$ ) and  $\Delta S$  ( $r = 0.177$ , 95% CI [0.080, 0.270],  $n = 284$ ), probably due to heterogeneity within the slicks or perhaps due to other complex processes in the slick areas. The weaker correlation to  $\Delta S$  is evident from Figure 2c as a more saline surface was detected between 02:00 UTC and 03:00 UTC as well between 04:10 UTC and 04:55 UTC despite EF FDOM above 4 and 10, respectively. Evaporation rates computed from meteorological bulk formulas increased after 02:00 UTC (Figure S4). The salty lens detected between 04:10 UTC and 04:55 UTC cannot be explained by our observations, for example, no increase in evaporation rates. Evaporation from water surfaces is a complex process, however, and evaporation rates from slicks may be controlled not only by the concentrations and types of film material but also because wave damping reduces the effective area (Garrett, 1971) or the wind profiles (Wu, 1971) over which evaporation can occur.

4. Conclusion

This study shows that concurrent high-resolution in situ measurements of SST and SSS are essential for better understanding SST and SSS dynamics. Our observations demonstrate that large cyanobacteria slicks complicate the evaluation of satellite-based SST and SSS, and therefore the prediction of regional warming and freshwater fluxes over the ocean. As remote sensing of salinity has become an international mission (i.e., SPURS, Salinity Processes in the Upper-ocean Regional Study; Lindstrom et al., 2015) to assess precipitation over the ocean, the wide coverage of the sea surface with biological slicks (Capone et al., 1998; Sieburth & Conover, 1965; Wurl et al., 2016) can bias satellite data with misinterpretation as having had recent precipitation. Aquarius and SMOS satellites retrieve microwave brightness temperature to obtain SSS from the upper 1 cm, equivalent to the penetration depth of the radiation, but its exponential decay at the sea surface leaves satellite measurements sensitive to changes in the skin layer (Yu, 2010). Synthetic aperture radar from satellites has the capability to detect slicks remotely (Espedal et al., 1998) and potentially useful to reduce the biases on SST and SSS reported here. The observed tendency of warmer SST across the upper 80  $\mu\text{m}$  compared to the upper 20  $\mu\text{m}$  indicates the need of real ground-truth in situ data, that is, from depth equivalent to penetration depth of satellite's IR or microwave radiation, to further advance retrieval algorithm for satellite-derived SST and SSS. Such improved assessment of climate variables from satellites is crucial to improve modeled forecasts on future ocean and climate change.

## Competing financial interests

The authors declare no competing financial interests.

## Acknowledgments

O. W. acknowledges funding by the European Research Council (ERC) project (grant GA336408). M. C. acknowledges funding through an MBA Research Fellowship, and K. B. was awarded a Natural Environment Research Council (NERC) EnvEast Doctoral Training Partnership PhD studentship. W. M. L. acknowledges funding from the Schmidt Ocean Institute and the Scientific Committee on Ocean Research (SCOR). C. J. Z. acknowledges funding by the Schmidt Ocean Institute (award SOI CU16-2285). All authors thank the Schmidt Ocean Institute for providing their research vessel *R/V Falkor* for the expedition AIR<sub>1</sub>SEA (cruise no. FK161010) and funding for open access fees. The captain, officers, and crew of the *R/V Falkor* are acknowledged for their invaluable support during the expedition. Cruise track and catamaran data of FK161010 are archived at the PANGAEA data publisher (Wurl et al., 2017) and available upon request (O. W.). C. J. Z. archives IR and polarimetric data products on Columbia Academic Commons (<https://academiccommons.columbia.edu/>), and raw imagery are available upon request. This is Lamont-Doherty Earth Observatory contribution number 8213.

## References

- Capone, D. G., Subramaniam, A., Montoya, J. P., Voss, M., Humborg, C., Johansen, A. M., et al. (1998). An extensive bloom of the N<sub>2</sub>-fixing cyanobacterium *Trichodesmium erythraeum* in the central Arabian Sea. *Marine Ecology Progress Series*, 172, 281–292. <https://doi.org/10.3354/meps172281>
- Capone, D. G., Zehr, J. P., Paerl, H. W., Bergman, B., & Carpenter, E. J. (1997). *Trichodesmium*, a globally significant marine cyanobacterium. *Science*, 276(5316), 1221–1229. <https://doi.org/10.1126/science.276.5316.1221>
- Comeau, A. M., Douglas, G. M., & Langille, M. G. (2017). Microbiome helper: A custom and streamlined workflow for microbiome research. *mSystems*, 2(1), e00127-16. <https://doi.org/10.1128/mSystems.00127-16>
- Conde, F. R., Churio, M. S., & Previtali, C. M. (2004). The deactivation pathways of the excited-states of the mycosporine-like amino acids shinorine and porphyra-334 in aqueous solution. *Photochemical & Photobiological Sciences*, 3(10), 960–967. <https://doi.org/10.1039/b405782a>
- Donlon, C. J., Minnett, P. J., Gentemann, C., Nightingale, T. J., Barton, I. J., Ward, B., & Murray, M. J. (2002). Toward improved validation of satellite sea surface skin temperature measurements for climate research. *Journal of Climate*, 15(4), 353–369.
- Donlon, C. J., Minnett, P. J., Jessup, A. T., Barton, I., Emery, W., Hook, S., et al. (2014). Ship-borne thermal infrared radiometer systems. *Experimental Methods in the Physical Sciences: Optical Radiometry for Ocean Climate Measurements*, 47(1), 305–404. <https://doi.org/10.1016/B978-0-12-417011-7.00011-8>
- Downing, H. D., & Williams, D. (1975). Optical constants of water in the infrared. *Journal of Geophysical Research*, 80(12), 1656–1661.
- Espedal, H. A., Johannessen, O. M., Johannessen, J. A., Dano, E., Lyzenga, D. R., & Knulst, J. C. (1998). COASTWATCH'95: ERS 1/2 SAR detection of natural film on the ocean surface. *Journal of Geophysical Research*, 103, 24,969–24,982. <https://doi.org/10.1029/98JC01660>
- Frew, N. M., Bock, E. J., Schimpf, U., Hara, T., Haußecker, H., Edson, J. B., et al. (2004). Air-sea gas transfer: Its dependence on wind stress, small-scale roughness, and surface films. *Journal of Geophysical Research*, 109, C08S17. <https://doi.org/10.1029/2003JC002131>
- Frka, S., Pogorzelski, S., Kozarac, Z., & Čosović, B. (2012). Physicochemical signatures of natural sea films from middle Adriatic stations. *The Journal of Physical Chemistry. A*, 25, 6552–6559. <https://doi.org/10.1021/jp212430a%2010.1021/jp212430a>
- Garrett, W. D. (1971). A novel approach to evaporation control with monomolecular films. *Journal of Geophysical Research*, 76, 5122–5123. <https://doi.org/10.1029/JC076i021p05122>
- Grossman, R. L., Bean, B. R., & Marlatt, W. E. (1969). Airborne infrared radiometer investigation of water surface temperature with and without an evaporation-retarding monomolecular layer. *Journal of Geophysical Research*, 74, 2471–2476. <https://doi.org/10.1029/JB074i010p02471>
- Harvey, G. W., & Burzell, L. A. (1972). A simple microlayer method for small samples. *Limnology and Oceanography*, 17(1), 156–157. <https://doi.org/10.4319/lo.1972.17.1.0156>
- Hühnerfuss, H., Alpers, W., & Richter, K. (1986). Discrimination between crude-oil spills and monomolecular sea slicks by airborne radar and infrared radiometer-possibilities and limitations. *International Journal of Remote Sensing*, 7(8), 1001–1013. <https://doi.org/10.1080/01431168608948905>
- Jarvis, N. L. (1962). The effect of monomolecular films on surface temperature and convective motion at the water/air interface. *Journal of Colloid Science*, 17(6), 512–522. [https://doi.org/10.1016/0095-8522\(62\)90019-3](https://doi.org/10.1016/0095-8522(62)90019-3)
- Jarvis, N. L., & Kagarise, R. E. (1962). Determination of the surface temperature of water during evaporation studies. A comparison of thermometer with infrared radiometer measurements. *Journal of Colloid Science*, 17(6), 501–511. [https://doi.org/10.1016/0095-8522\(62\)90018-1](https://doi.org/10.1016/0095-8522(62)90018-1)
- Jessup, A. T., Asher, W. E., Atmane, M., Phadnis, K., Zappa, C. J., & Loewen, M. R. (2009). Evidence for complete and partial surface renewal at an air-water interface. *Geophysical Research Letters*, 36, L16601. <https://doi.org/10.1029/2009GL038986>
- Kahru, M., Horstmann, U., & Rud, O. (1994). Satellite detection of increased cyanobacteria blooms in the Baltic Sea: Natural fluctuation or ecosystem change? *Ambio*, 23, 469–472.
- Kahru, M., Leppanen, J. M., & Rud, O. (1993). Cyanobacterial blooms cause heating of the sea surface. *Marine Ecology Progress Series*, 101, 1/2, 1–1/2, 7.
- Katsaros, K. (1980). Radiative sensing of sea surface temperature. In F. Dobson, L. Hasse, & R. Davis (Eds.), *Air Sea Interaction: Instruments and Methods* (pp. 293–317). New York: Plenum Press. [https://doi.org/10.1007/978-1-4615-9182-5\\_17](https://doi.org/10.1007/978-1-4615-9182-5_17)
- La Mer, V. K., & Healy, T. W. (1965). Evaporation of water: Its retardation by monolayers. *Science*, 148(3666), 36–42. <https://doi.org/10.1126/science.148.3666.36>
- Levitus, S., Antonov, J. I., Boyer, T. P., Baranova, O. K., Garcia, H. E., & Zweng, R. A. L., et al. (2012). World ocean heat content and thermosteric sea level change (0–2000 m), 1955–2010. *Geophysical Research Letters*, 39, L10603. <https://doi.org/10.1029/2012GL051106>
- Lindstrom, E., Bryan, F., & Schmitt, R. (2015). SPURS: Salinity Processes in the Upper-Ocean Regional Study: The North Atlantic Experiment. *Oceanography*, 28(1), 14–19. <https://doi.org/10.5670/oceanog.2015.01>
- Marmorino, G. O., & Smith, G. B. (2006). Reduction of surface temperature in ocean slicks. *Geophysical Research Letters*, 33, L14603. <https://doi.org/10.1029/2006GL026502>
- Martin, S. (2014). *An introduction to ocean remote sensing* (2nd ed.). New York: Cambridge University Press.
- McLeish, W., & Putland, G. E. (1975). Measurements of wind-driven flow profiles in the top millimeter of water. *Journal of Physical Oceanography*, 5(3), 516–518.
- Price, J. F., Weller, R. A., & Pinkel, R. (1986). Diurnal cycling: Observations and models of the upper ocean response to diurnal heating, cooling, and wind mixing. *Journal of Geophysical Research*, 91, 8411–8427. <https://doi.org/10.1029/JC091iC07p08411>
- Ribas-Ribas, M., Mustaffa, N. I. H., Rahlff, J., Stolle, C., & Wurl, O. (2017). Sea Surface Scanner (S<sup>3</sup>): A catamaran for high-resolution measurements of biogeochemical properties of the sea surface microlayer. *Journal of Atmospheric and Oceanic Technology*, 34(7), 1433–1448. <https://doi.org/10.1175/JTECH-D-17-0017.1>
- Romano, J. C. (1996). Sea-surface slick occurrence in the open sea (Mediterranean, Red Sea, Indian Ocean) in relation to wind speed. *Deep Sea Research, Part I*, 43(4), 411–423. [https://doi.org/10.1016/0967-0637\(96\)00024-6](https://doi.org/10.1016/0967-0637(96)00024-6)
- Saunders, P. M. (1967). The temperature at the ocean-air interface. *Journal of the Atmospheric Sciences*, 24(3), 269–273. [https://doi.org/10.1175/1520-0469\(1967\)024%3C0269:TTATOAA%3E2.0.CO;2](https://doi.org/10.1175/1520-0469(1967)024%3C0269:TTATOAA%3E2.0.CO;2)
- Sieburth, J. M. N., & Conover, J. T. (1965). Slicks associated with *Trichodesmium* blooms in the Sargasso Sea. *Nature*, 205(4973), 830–831. <https://doi.org/10.1038/205830b0>

- Sinha, R. P., Klisch, M., Gröniger, A., & Häder, D.-P. (1998). Ultraviolet-absorbing/screening substances in cyanobacteria, phytoplankton and macroalgae. *Journal of Photochemistry and Photobiology B: Biology*, 47(2-3), 83–94. [https://doi.org/10.1016/S1011-1344\(98\)00198-5](https://doi.org/10.1016/S1011-1344(98)00198-5)
- Soloviev, A., & Lukas, R. (2006). *The near-surface layer of the ocean*. Dordrecht: Kluwer Academic.
- Song, Y. T., Lee, T., Moon, J.-H., Qu, T., & Yueh, S. (2015). Modeling skin-layer salinity with an extended surface-salinity layer. *Journal of Geophysical Research: Oceans*, 120, 1079–1095. <https://doi.org/10.1002/2014JC010346>
- Taylor, J. D., Cottingham, S. D., Billinge, J., & Cunliffe, M. (2014). Seasonal microbial community dynamics correlate with phytoplankton-derived polysaccharides in surface coastal waters. *The ISME Journal*, 8(1), 245–248. <https://doi.org/10.1038/ismej.2013.178>
- Tilstone, G. H., Ains, R. L., Vicente, V. M., Widdicombe, C., & Llewellyn, C. (2010). High concentrations of mycosporine-like amino acids and colored dissolved organic matter in the sea surface microlayer off the Iberian Peninsula. *Limnology and Oceanography*, 55(5), 1835–1850. <https://doi.org/10.4319/lo.2010.55.5.1835>
- Wu, J. (1971). Evaporation retardation by monolayers: Another mechanism. *Science*, 174(4006), 283–285. <https://doi.org/10.1126/science.174.4006.283>
- Wurl, O., Miller, L., & Vagle, S. (2011). Formation and distribution of transparent exopolymer particles in the ocean. *Journal of Geophysical Research*, 116, C00H13. <https://doi.org/10.1029/2011JC007342>
- Wurl, O., Mustafa, N. I. H., & Ribas-Ribas, M. (2017). Multiparameter measurement of biochemical properties of the sea surface microlayer in the Pacific Ocean during R/V Falkor cruise FK161010. *PANGAEA*. <https://doi.org/10.1594/PANGAEA.882430>
- Wurl, O., Stolle, C., Van Thuoc, C., Thu, P. T., & Mari, X. (2016). Biofilm-like properties of the sea surface and predicted effects on air-sea CO<sub>2</sub> exchange. *Progress in Oceanography*, 144, 15–24. <https://doi.org/10.1016/j.pocean.2016.03.002>
- Yu, L. (2010). On sea surface salinity skin effect induced by evaporation and implications for remote sensing of ocean salinity. *Journal of Physical Oceanography*, 40(1), 85–102. <https://doi.org/10.1175/2009JPO4168.1>
- Zappa, C. J., Banner, M. L., Schultz, H., Corrada-Emmanuel, A., Wolff, L. B., & Yalcin, J. (2008). Retrieval of short ocean wave slope using polarimetric imaging. *Measurement Science and Technology*, 19(5), 055503. <https://doi.org/10.1088/0957-0233/19/5/055503>
- Zappa, C. J., Banner, M. L., Schultz, H., Gemmrich, J. R., Morison, R. P., LeBel, D. A., & Dickey, T. (2012). An overview of sea state conditions and air-sea fluxes during RaDyO. *Journal of Geophysical Research*, 117, C00H19. <https://doi.org/10.1029/2011JC007336>
- Zhang, Y., & Zhang, X. (2012). Ocean haline skin layer and turbulent surface convections. *Journal of Geophysical Research*, 117, C04017. <https://doi.org/10.1029/2011JC007464>
- Zhou, Y., Jiang, L., Lu, Y., Zhan, W., Mao, Z., Qian, W., & Liu, Y. (2017). Thermal infrared contrast between different types of oil slicks on top of water bodies. *IEEE Geoscience and Remote Sensing Letters*, 14(7), 1042–1045. <https://doi.org/10.1109/LGRS.2017.2694609>